Oil Shale, 2002, Vol. 19, No. 4
pp. 373-386
ISSN 0208-189X

https://doi.org/10.3176/oil.2002.4.03

INVESTIGATION OF THE MINERAL COMPOSITION OF ESTONIAN OIL-SHALE ASH USING X-RAY DIFFRACTOMETRY

A. PAAT, R. TRAKSMAA

Centre for Materials Research,
Tallinn Technical University
5 Ehitajate Rd., Tallinn, 19086 Estonia

The mineral composition of ashes from oil shale power plants was determined by X-ray diffractometry using modern software and databases. Changes in the whole ash as well as its fractions were observed throughout the ash-handling system.

Introduction

As stated in our previous paper [1], knowing the mineral composition of Estonian oil shale ash contributes to more effective use of boilers in oil-shale-fired power plants (PP), better handling of environmental pollution problems and enhancing practical utilization of ashes. Only the method of X-ray diffraction (XRD) analysis allows direct spectrum-based determination of the mineral and phase composition of the investigated material, as well as its composition in terms of chemical compounds, using the respective databases.

While in industrial oil-shale-fired boilers the chemical composition of the ashes produced can be calculated on the basis of data from laboratory experiments and technical analysis [2, 3], this is impossible in various nodes of the gas duct due to separation of ashes. Thus, the composition of ashes from different parts of the gas duct can be determined only by direct analyses.

The aim of the current research was to determine the mineral composition of ashes from Estonian PP (EPP) using the method of XRD. Ash samples were collected according to the scheme in Fig. 1. Up-to-date X-ray diffractometer with respective databases and software were used. An attempt was made to determine the mineral composition of ash and follow its changes along the nodes of the ash-handling system. In the first stage of the research, only qualitative analysis was used, ignoring the X-ray amorphous part.

Experimental

XRD data were collected on a *Bruker AXS* diffractometer D5005 with scintillation detector. Theta-theta geometry, Cu tube, variable divergence and antiscattering slits and diffracted beam graphite monochromator were used. The goniometer, its accessories, and the detector were microprocessor-controlled. The alignment of the diffractometer was carried out under computer control. Data acquisition and data evaluation was achieved with a high-performance software package *DIFFRAC*^{plus}. For identification of crystalline phases, the Powder Diffraction Database (PDF-2) of the International Centre for Diffraction Data, release 1997, was used. For identification of phases, different automatic and manual search methods, facilitated by the special software to the diffractometer and database, were combined.

For measuring X-ray diffractograms the following parameters were used: tube current 40 mA, tube voltage 40 kV, step size 0.02 or 0.04°, time per step 10 or 20 s, 2Θ 15–70 or 11–80°, rotating object. Measurements of shorter duration (0.04°, 10 s, 15–70°) were used for following the qualitative mutations in the main compounds of the ashes, measurements of longer duration (0.02°, 20 s, 11–80°) were used to identify low-quantity compounds. For determining the content of the major compounds, two samples were prepared from the same ash, so the detected content was the average of those two. The results of the two measurements did not differ significantly. The samples were mostly prepared in standard sample holders. The amount of ashes of some fractions was too small to fill the standard sample holder. In this case, a self-made low holder was used, where the ash was prepared on the X-ray amorphous tape.

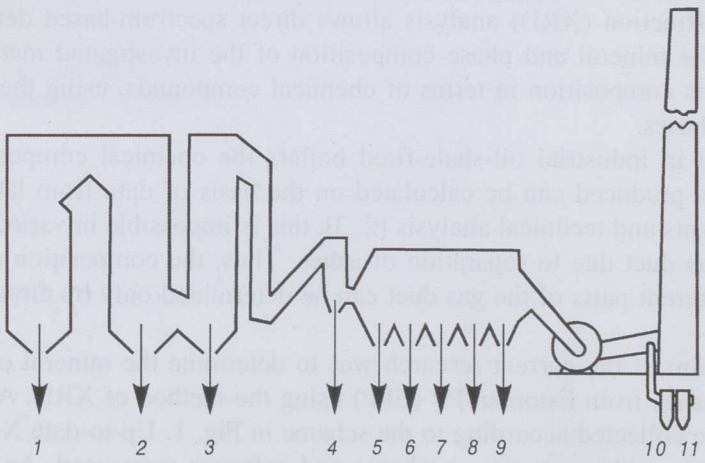

Fig. 1. Scheme of ash sampling: *1* – furnace bottom; gas duct: *2* – superheater, *3* – economizer; *4* – cyclone; electrostatic precipitators: *5* – prechamber, *6* – field I, *7* – field II, *8* – field III, *9* – field IV; flue: *10* – cyclone, *11* – cloth filter

The ash from the boiler K-3A of EPP was studied. During the sample taking, the boiler's working conditions were as follows: steam production 235 t/h, superheated steam pressure 135 kgf/cm^2 and temperature 535 °C.

Figure 1 shows the scheme of ash sampling at EPP. The same figure also presents the fly ash sampling points at Baltic PP (BPP): the collecting cyclone *10* located after the draft fan and the cloth filter *11* after them. So, the ashes examined were those of EPP: *1–9*; and those of BPP: *10* and *11*.

EPP ash samples were fractioned by dry sieving. Sieves with sieve mesh of 45 μm and 1 mm were used. The fractions were classified as follows: fine fraction – ash particle maximum size below 45 μm, coarse fraction – particles from 45 μm to 1 mm, and the coarsest fraction – with particle size above 1 mm. Unfractioned ash is also called the whole ash. The coarser ash particles were ground before X-ray measurements in an agate mortar.

As ash contains also ferrite (Fe_2O_3, Fe_3O_4) or antiferromagnetic (FeO, FeS, FeOOH, $FeCO_3$) particles, strong permanent magnet was used to enrich ash with those compounds for their more veracious identification. However, it has to be considered that iron oxides also bind particles together and thus inhibit dispersion of the mineral particles [2].

Results and Discussion

Ash Fractions

The fractionation results are given in the Table. The coarsest ash (slag) could be found only in furnace and superheater ash, and its content was small, especially in the furnace ash. The diversity of gas duct ashes was considerable: the ash collected from under the economizer was much coarser than the superheater ash. Surprising was the large amount of coarse fraction in electrostatic precipitator ash, especially in the ash of field I – even 6.4 %. Along the following fields it diminished but to some extent coarse particles

Share of Different-Size Ash Particles, %

Ash type	Fraction		
	Fine, < 45 μm	Coarse, 45 μm – 1 mm	Coarsest, >1 mm
Furnace bottom ash	6.4	93.6	<0.1
Superheater ash	19.2	80.0	0.8
Economizer ash	4.8	95.2	–
Cyclone ash	33.8	66.2	–
Electrostatic precipitators:			
Prechamber ash	94.4	5.6	–
Field I ash	93.6	6.4	–
Field II ash	97.4	2.6	–
Field III ash	98.4	1.6	–
Field IV ash	99.6	0.4	–

penetrated up to field IV. Detection of coarse particles in electrostatic precipitator ash was noted in the case of both 4th-stage boilers of BPP [5] as well as in the ash from EPP [6], where this was attributed to poor performance of electrostatic precipitators. Still, the large amount of coarse particles was surprising.

X-Ray Spectrums of the Ashes

Spectrums of all eleven ashes are given in crude form in Fig. 2. The figure also gives the formulas of chemical compounds corresponding to the more intensive lines of the spectrum. For most of the compounds, the change in their relative content along the ash-handling system could be easily observed.

All the spectrums showed clearly distinguishable lines of lime CaO (PDF pattern 37-1497), anhydrite $CaSO_4$ (37-1496), quartz SiO_2 (46-1045), periclase MgO (45-946) and calcite $CaCO_3$ (5-586). (In brackets the PDF pattern numbers, which match the chemical compound under examination best, are given; i.e. numbers which in the case of automatic search gave minimal figure of merit and in manual search matched best the position and intensity of experimental spectrum lines.) From the furnace to field IV of the electrostatic precipitator dicalcium silicate ($2CaO \cdot SiO_2$) lines could be observed, though they were poorly distinguishable since they mostly coincided with the strong lines of the above-mentioned minerals. The quest system preferred larnite β-Ca_2SiO_4 (33-302) here. The lines of sylvite KCl (41-1476) could be detected in the electrostatic precipitator and flue ashes (also very faintly in furnace ashes).

Main Minerals in Ashes

For estimating the mineral content of the ashes, the intensity (cps) of each one's first (the most intensive) line was registered and their changes observed. As larnite's first line coincided with lime's intensive line, the intensity of its second line was determined and reduced to the first line intensity.

Figure 3 presents the changes in the X-ray line intensity for the six main minerals found in the ash of the EPP's ash-handling system, from furnace to electrostatic precipitator field IV, in the whole ash and in the fractions. The same figure gives the intensity of the X-ray lines for the non-fractioned ashes of BPP in a separate segment.

Figure 4 shows the changes in the mineral composition of these ashes by fractions – fine and coarse fraction and non-fractioned ash (the whole ash). The figures show that the composition of flue ash is not a smooth continuation of that of the electrostatic precipitator ash. It means that the ashes of Estonian and Baltic PP are different. The same result was gained while comparing an X-ray spectrum of the control sample of ashes taken from the BPP electrostatic precipitator field IV to that of analogous ash from EPP.

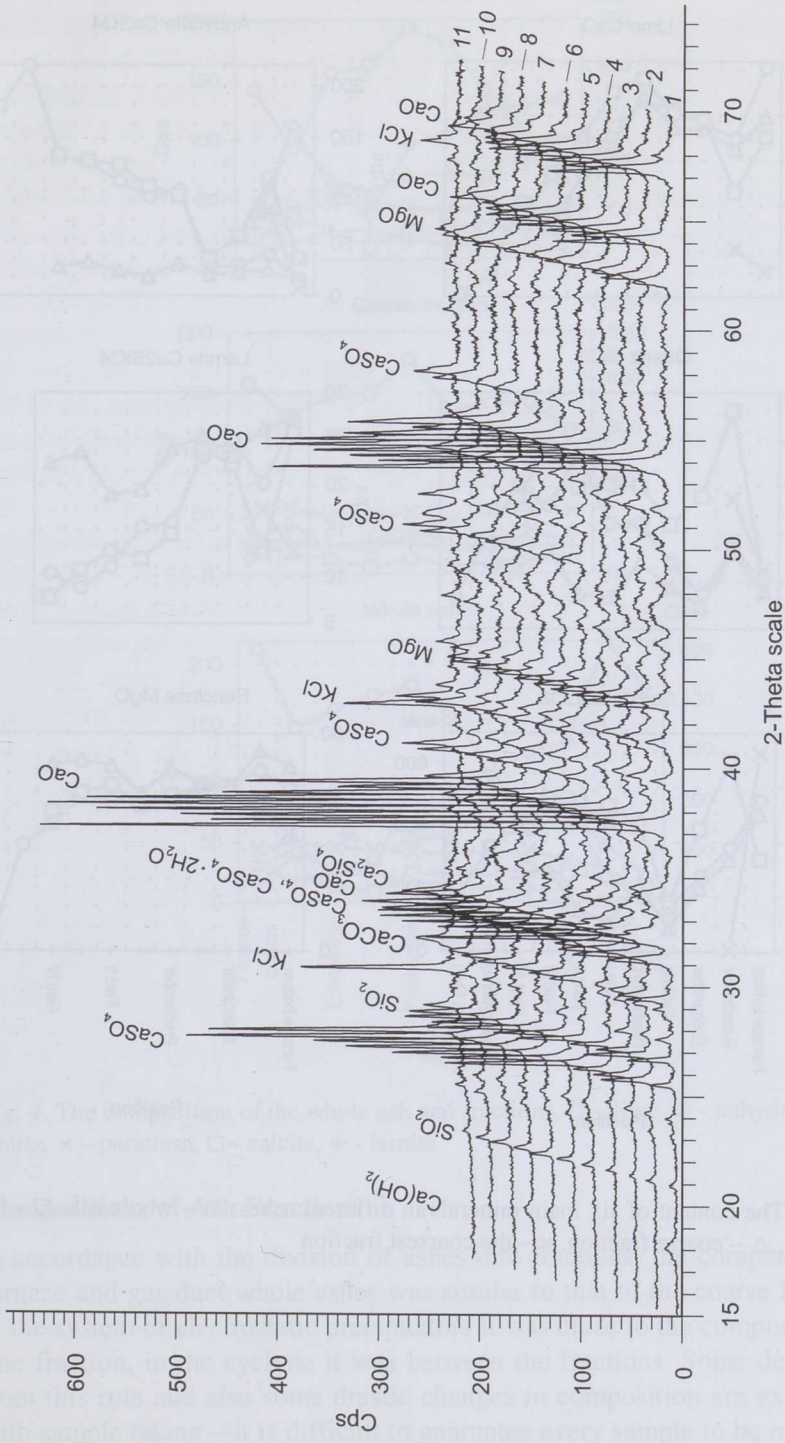

Fig. 2. X-ray spectrums of eleven ashes. For the legend see Fig. 1

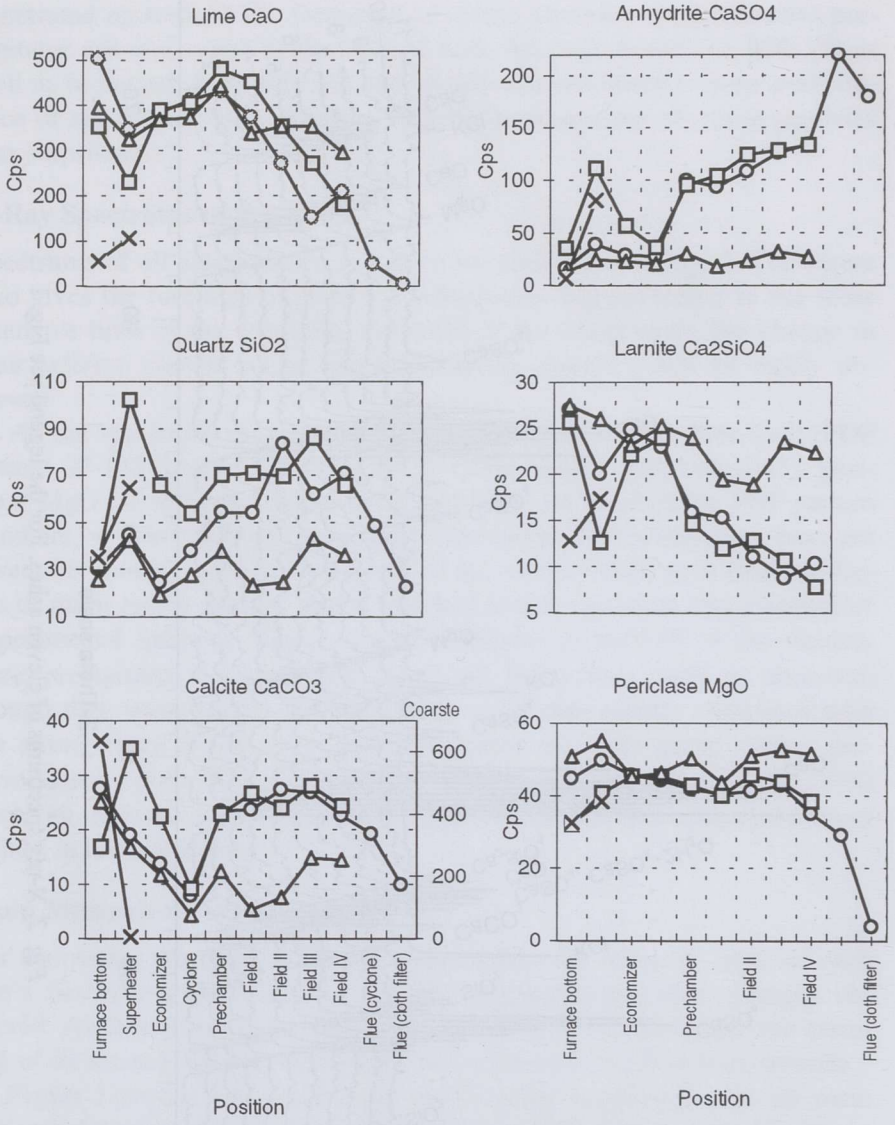

Fig. 3. The content of six main minerals in different ashes: ○ – whole ash, □ - fine fraction, △ – coarse fraction, × – the coarsest fraction

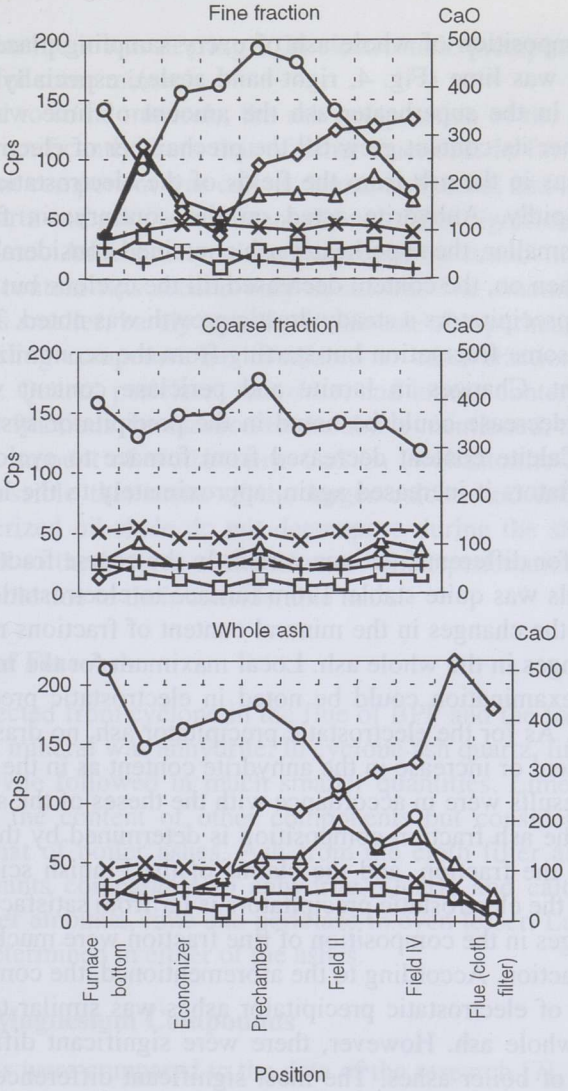

Fig. 4. The composition of the whole ash and fractions. ○ – lime, ◇ - anhydrite, △ – quartz, × – periclase, □ - calcite, + - larnite

Compositions of Ash Fractions

In accordance with the division of ashes into fractions, the composition of furnace and gas duct whole ashes was similar to that of the coarse fraction, in the system of electrostatic precipitators it was close to the composition of fine fraction, in the cyclone it was between the fractions. Some deviations from this rule and also some drastic changes in composition are explicable with sample taking – it is difficult to guarantee every sample to be representative.

In the composition of whole ash of every sampling place, the predominant mineral was lime (Fig. 4, right-hand scale), especially in the case of furnace ash. In the superheater ash the amount of lime was considerably smaller, further its content grew till the prechamber of electrostatic precipitators, whereas in the ash from the fields of the electrostatic precipitator it decreased rapidly. Anhydrite acted on the contrary: in furnace ash its amount was smaller, the superheater ash contained considerably more anhydrite. From then on, the content decreased till the cyclone but throughout the electrostatic precipitators a steady drastic growth was noted. The quartz content showed some fluctuation but starting from the economizer the increase was prevalent. Changes in larnite and periclase content were relatively small, some decrease could be noted in the precipitator system, especially for larnite. Calcite content decreased from furnace to cyclone, in electrostatic precipitators it increased again, approximately to the level of the furnace.

The data for different fractions varied. In the coarse fraction the content of all minerals was quite stable. From furnace to electrostatic precipitator's prechamber, the changes in the mineral content of fractions repeated the respective changes in the whole ash. Local maximum for the majority of minerals under examination could be noted in electrostatic precipitator's prechamber ash. As for the electrostatic precipitator ash, no drastic decrease in the lime content or increase in the anhydrite content as in the whole ash was noted. The results were in accordance with the theses of the school of Kikas stating that the ash fraction composition is determined by the size of particles forming the fraction, and the claims of the Finnish scientists that the efficiency of the electrostatic precipitators is far from satisfactory [6].

The changes in the composition of fine fraction were much bigger than in the coarse fraction. According to the aforementioned, the composition of the fine fraction of electrostatic precipitator ashes was similar to the composition of the whole ash. However, there were significant differences in the composition of boiler ashes. The most significant differences occurred between superheater and furnace ash, to a smaller extent also between superheater and economizer ash. Furnace ash and economizer ash were more similar in their composition. The latter referred also to the coarse fraction and the whole ash.

The results obtained for fractions were generally in accordance with earlier analyses. A more detailed comparison was, unfortunately, not possible as different research teams had used fractions with different particle size; and several ashes which seemed to have been of less interest had therefore been studied less. A number of studies on the composition of fractions had been carried out for the cyclone ash from BPP. As shown in Fig. 3, the differences in the mineral content of ash fractions in EPP were the smallest in cyclone ash. The ratio of the content of a certain compound in fine and coarse ash fractions was nearing 2 for anhydrite, quartz and calcite; for lime,

periclase and larnite it was nearing 1. In electrostatic precipitators this ratio could reach 5 for some minerals.

With regard to some minerals, the ash composition of the coarsest fraction differed significantly from that of other fractions. In furnace ash slag, the predominant component was calcite. Lime, anhydrite, and larnite content was small. Quartz and periclase content did not differ significantly from this of other fractions. Additionally, dolomite could be found in considerable amounts – its content was second only to calcite. The amount of dolomite and calcite was smaller, barely notable, in the ash of superheater slag. Lime was the prevailing compound but compared to other fractions its amount was still small. Quartz, periclase, anhydrite, and larnite content was similar to this of other fractions. In addition to the above-mentioned, there was also a considerable amount of wollastonite $CaSiO_3$ (wollastonite-2M, PDF 27-0088). It is possible that some of the larger calcite and dolomite pieces found in pulverized oil shale do not decompose during the short period in furnace and fall to the bottom of the furnace. Their penetration into the gas duct is impossible due to their considerable mass.

Composition of Flue Ash

In the ash collected from cyclone in the flue of BPP and the following cloth filter, the main mineral was anhydrite. In cyclone ash quartz, lime, periclase, calcite and sylvite followed in much smaller quantities. Lime content was comparable to the content of other components but considerably smaller compared to that of boiler ashes. Ash from the cloth filter also contained sylvite in amounts comparable to anhydrite. Quartz and calcite were detected in smaller amounts, lime and periclase in even lesser. Larnite content could not be determined in either of the ashes.

Calcium and Magnesium Compounds

Here our results were compared to the data of the research [7]. In that study, all the types of fly ashes from BPP were determined by powder XRD. Before actual analysis the samples were stored several years under atmospheric conditions.

The calcareous minerals calcite and dolomite found in oil shale decomposed in furnace and formed oxides – lime and periclase. A number of base minerals did not decompose and fell to the bottom of the furnace – this was shown by the high content of these minerals in the coarsest furnace ash. Differently from the research [7], we did not find dolomite in detectable amounts in other ash fractions. The oxides formed carbonized and sulfatized forming calcite, magnesite, anhydrite and gypsum. Calcite could be found in all ash fractions but it could not be claimed to decrease constantly along the gas duct. The lines of magnesite did exist on the roentgenogram but were too weak to allow its quantitative determination. In general, determining

magnesite in kukersite ash is difficult as its strongest lines overlap with the lines of the main compounds of ash.

The situation with sulfate compounds was of a particular kind. As a result of sulfatization of calcium oxide anhydrite, gypsum or both were found from the kukersite ash. It has to be considered that in humid environment anhydrite binds water and forms gypsum. Our X-ray spectrums showed the existence of anhydrite in all ash samples studied; in the system of electrostatic precipitators it ranged second after lime, while in flue it was overwhelmingly the first. Gypsum content, on the contrary, slightly exceeded that of anhydrite in furnace, gas duct and cyclone ash. Gypsum could not be detected in the first fields of precipitators, and in the last fields its amount was small. Processed X-ray spectrums near $2\Theta = 31°$ of ashes in Fig. 5 illustrate the aforementioned fact. (Background has been disintegrated from spectrums, Kα2 lines eliminated, and Fourier transformation performed.) The figure depicts the most intensive line of gypsum (100 %), the second line of anhydrite (26 %) and on the left very weak line of larnite close to one another.

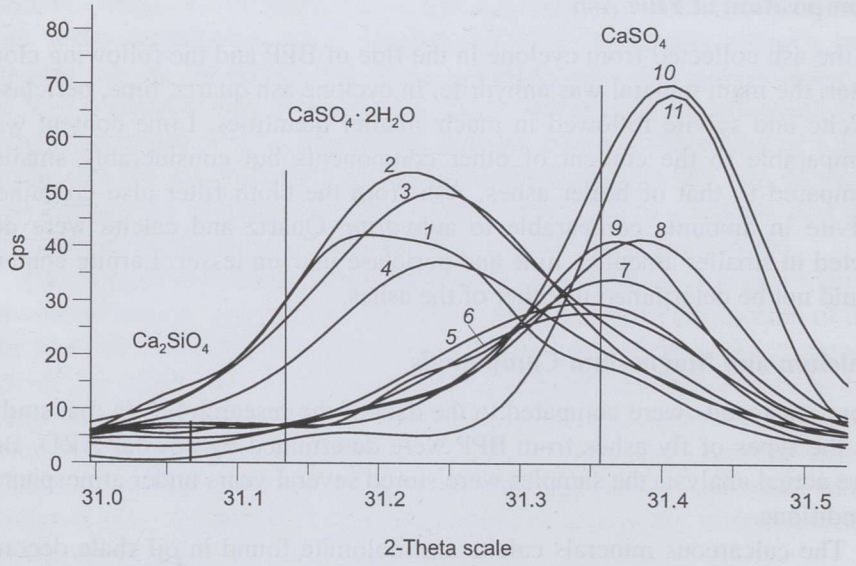

Fig. 5. The peaks of gypsum and anhydrite near $2\Theta = 31°$. For the legend see Fig. 1

If gypsum is heated, bassanite $CaSO_4 \cdot 1/2H_2O$ may form. Generally, bassanite lines appear in the kukersite ash X-ray spectrums with very low intensity, except for the ash caught by the cloth filter, where its amount is considerable.

Some of the lime may react with water vapour forming portlandite. For the ashes investigated, portlandite lines appeared in the spectrums of furnace, III, II and I fields of the electrostatic precipitator and flue ashes.

Figure 5 shows that the experimental maximum intensity locations did not coincide with those given in the database. This is characteristic to calcium compounds in kukersite ash. Several small shifts in peaks were not systematic and could be attributed to deviations in sample preparation. Some systematic and substantial shifts also occurred. The most significant shifts were noted for dolomite peaks, and these occurred towards bigger interplanar spacing *d*. To get PDF values the experimental values of *d* had to be multiplied by 1.0035 ($d \times By$). The peaks of lime had shifted towards the lower value of *d*: $d \times By$ = 0.9990–0.9993 in all the ashes. The shift increased along the ash-handling system from furnace to flue. The shifts in peaks can be attributed to the behaviour of calcium and magnesium ions: in lime calcium is partially substituted by magnesium and in dolomite *vice versa*.

Other calcium compounds present in kukersite ash are probably hydropholite $CaCl_2$ and oldhamite CaS. Potassum calcium sulfate $K_2Ca_2(SO_4)_3$ is the most probable mixed sulfate of calcium and potassium.

Iron Compounds

As for iron oxides, kukersite ash contained hematite Fe_2O_3 and magnetite Fe_3O_4. Magnetite could be detected only in ash pretreated with magnet (pretreatment with magnet strengthened the peak intensity of both compounds 2-3 times). The peaks of iron sulfides were very feeble. Automatic search systems gave troilite-2H FeS first in all ashes, whereas magnetic treatment could be detected. Occurrence of marcasite FeS_2 was also probable, but pyrite FeS_2 could not be identified. The presence of siderite $FeCO_3$ and iron sulfate $Fe_2(SO_4)_3$ was also probable.

Cement Minerals

As for calcium silicates, kukersite ash contained the above-mentioned larnite Ca_2SiO_4 (dicalcium silicate $2CaO \cdot SiO_2$) and wollastonite-2M $CaSiO_3$ (monocalcium silicate $CaO \cdot SiO_2$). Of calcium iron oxides, srebrodolskite $Ca_2Fe_2O_5$ (dicalcium ferrite $2CaO \cdot Fe_2O_3$) was probable. Of calcium aluminates calcium aluminium oxide $CaAl_2O_4$ (monocalcium aluminate $CaO \cdot Al_2O_3$) was found, and occurrence of calcium aluminium oxide $Ca_3Al_2O_6$ (tricalcium aluminate $3CaO \cdot Al_2O_3$) was probable. Here it could be stated that monocalcium aluminate matched best the PDF file marked Q (questionable).

Feldspars, Micas and Other Silicates

Orthoclase $KAlSi_3O_8$ and microcline $KAlSi_3O_8$ probably represented potassium feldspars; as for sodium and calcium feldspars, the compounds containing pure Na like albite $NaAlSi_3O_8$ and pure Ca like anorthite $CaAl_2Si_2O_8$ were detected, also ordered sodium anorthite $(Ca,Na)(Al,Si)_2Si_2O_8$. Biodite

$KMg_3Si_3AlO_{10}(OH)_2$ and muscovite $KAl_2Si_3AlO_{10}(OH,F)_2$ represented mica. The most probable representative of melites is gehlenite $Ca_2Al_2SiO_7$. In small amounts epidotes $Ca_2(Al,Fe)_3(Si_2O_7)(SiO_4)(OH)_2$ could occur.

Potassium Compounds

In addition to the aforementioned sylvite and potassium calcium sulfate, arcanite K_2SO_4 might also occur.

Other Compounds

As for titanium oxides TiO_2, rutile and possibly also brookite could be found, but the occurrence of anatase is of low probability. Zirconium occurred in silicates – zircon $ZrSiO_4$ and zirconium silicate $ZrSi_{24}O_{50}$ are probably represented.

Background

Kukersite ash always contained X-ray amorphous substance, consequently its X-ray spectrum had background. In general, the intensity of background grew along the gas duct from furnace to flue ash. Superheater ash was an exception, its background being comparable to that of cyclone ash. Characteristic to the background of kukersite ash was its broad maximum at $2\Theta =$ $= 31–34°$. Utsal reports similar maximum for ashes of Syrian oil shale [8], which is characteristic to glass-like inorganic X-ray amorphous phase.

Stability of the Ash

As the changes in the composition of kukersite ash in time are generally known, experiments were made to determine them. A new XRD measurement was made for the ash of IV field of electrostatic precipitator which had been kept on silica gel in the desiccator for 21 months. The comparison of the diffractograms with the previous ones revealed astonishingly small changes in the composition of the ash – only the intensity of peaks for lime CaO had decreased by a few per cent, changes in the peaks of other compounds did not exceed random deviation.

Next, the ash was kept in a humid environment (relative humidity 85 %) for 4.7 months. This caused the intensity of peaks for lime to decrease *ca* ten times and strong peaks of portlandite to appear, also strengthening of calcite peaks was perceptible.

Similar changes occurred if furnace ash was kept in humid environment and as furnace ash contains large quantities of lime, the changes in the diffractogram were especially significant.

No significant changes in gypsum and anhydrite content were noted for either of the ashes.

Because of difference in the storing conditions the mineral composition of ashes differed from those reported in [7].

Conclusions

The results of ash fractioning showed high concentration of coarse particles in the ash from electrostatic precipitators.

The contemporary X-ray diffraction hard- and software allows effective investigation of mineral or phase composition of ash (and oil shale). In the current research, *ca* forty chemical compounds/minerals were identified in kukersite ash. *Ca* ten of them could be quantitatively determined without additional processing, *ca* ten were clearly identifiable and *ca* twenty "probably occur"; processing the ashes would facilitate their firmer identification.

The investigations accomplished showed considerable differences in the compositions of ash fractions. For the first time the changes in the content of the six main minerals were observed throughout the whole ash-handling system. For every mineral, the changes were different and not smooth. The common trend was the increase in anhydrite content and decrease in lime content along the ash-handling duct.

In absolutely water-free environment kukersite ash can be preserved without changes in its composition; humid atmosphere causes essential changes in the composition.

Acknowledgments

The authors are grateful to Rein Rootamm for assistance by sampling of the kukersite ash.

REFERENCES

1. *Paat, A.* About the mineral composition of the Estonian oil shale ash // Oil Shale. 2002. Vol. 19, No. 3. P. 333–345.
2. *Rootamm, R., Õispuu, L.* Berechnung der chemischen Zusammensetzung des Brennschiefers und dessen Asche auf Grund der Angaben von technischen Analysen // Trans. Tallinn Tech. Univ. 1994. No. 739. P. 68–78 [in Estonian, summary in German].
3. *Arro, H., Prikk, A., Pihu, T.* Calculation of composition of Estonian oil shale and its combustion products on the basis of heating value // Oil Shale. 1998. Vol. 15, No. 4. P. 339–340.
4. *Moore, D.M., Reynolds, R.C.* X-ray Diffraction and the Identification and Analysis of Clay Minerals. – Oxford Univ., 1997.
5. *Veretevskaja, I., Galibina, E.* The composition and properties of oil shale ash from boilers of 4th stage of Baltic TPP // Studies on Building. 9. Tallinn, 1968. P. 106–113 [in Russian].

6. *Aunela, L., Häsänen, E., Kinnunen, V., et al.* Emissions from oil shale power plants // Oil Shale. 1995. Vol. 12, No. 2. P. 165–177.
7. *Pets, L.* Probable modes of occurrence of trace elements in oil shale ashes of power plant // Oil Shale. 1999. Vol. 16, No. 4S. P. 464–472 [in Russian, summary in English].
8. *Utsal, K.* Investigation of the mineral and organic composition of Syrian oil shales by X-ray diffraction method // Oil Shale. 1987. Vol. 4, No. 2. P. 188–199.

Presented by J. Kann
Received January 18, 2002